

# From oceanographic to acoustic forecasting: acoustic model calibration using in situ acoustic measures

Nélson Martins and Sérgio M. Jesus\*

## Abstract

Sonar performance prediction relies heavily on acoustic propagation models and environmental representations of the oceanic area in which the sonar is to operate. The performance estimate is derived from a predicted acoustic field, which is the output of a propagation model. Though well developed nowadays, acoustic propagation modeling is limited in practice by simplifications in the numerical methods, in the environmental structure to consider (for computational reasons), and even in the knowledge of some environmental properties. This is complicated by the fact that, in sonar performance prediction, the environmental properties need to be predicted for a far future, in the order of hours or days. These limitations imply that the acoustic field at the output of the acoustic predictor is biased, in current methods. In mathematical terms, the prediction of the acoustic field can be seen as a model parametrization problem, in which the model is a numerical propagation model, and the parameters are environmental descriptors which, when fed to the propagation model, best model the future acoustic field. Since the 1980's, significant research has been done in the development of propagation model parametrization, using techniques of the so-called "acoustic inversion" family. These techniques, having as objective the estimation of environmental properties of an oceanic area, use observed acoustic fields at the area, to be matched with candidate fields corresponding to candidate environmental pictures. At the end, the best acoustic match gives the estimated environment, in other words, the best model parameters to closely reproduce the measured acoustic field. In the current work, the technique of acoustic inversion is used in the design of an acoustic predictor, together with oceanographic forecasts and measures. Synthetic acoustic data generated with oceanographic measures taken in the MREA'03 sea trial, is used to illustrate the proposed method. The results show that a collection of environments estimated by past acoustic inversions, can ameliorate the acoustic estimates for future time, as compared to a conventional method.

**Keywords:** acoustic inversion, acoustic prediction, Bayesian estimation, oceanographic forecast, rapid environmental assessment

## 1 Introduction

The problem of estimating the acoustic field in a given oceanic area at a future time has triggered research in both areas of oceanography and underwater acoustics[1, 2].

---

\*Institute for Systems and Robotics, University of Algarve, 8005-139 Faro, Portugal, {nmartins, sjesus}@ualg.pt

Taking into account the strong dependence of acoustic propagation on the space-time-dependent sound speed field, the oceanographic community developed sophisticated oceanographic prediction tools[3, 4, 5]. These tools combine physics, statistics and data models, giving estimates of the temperature, salinity and currents fields evolution, among others[5]. The acoustics community developed acoustic propagation models based on *e.g.* normal mode theory, ray theory, fast field program, or the parabolic equation, which give accurate predictions of the acoustic field[2]. These models take environmental quantities as input, giving an acoustic field estimate as output.

The fact that the dependence of acoustic signals on environmental conditions is highly nonlinear prevents for the definition of models of the acoustic field evolution and consecutive tracking by time-marching algorithms. Thus, it is a common practice to run a calibrated ocean dynamic model to produce sound speed forecasts for the area of interest, and use those along with geometric/geoacoustic archival data as input to an acoustic propagation model[6]. A robust prediction system, including feedback, is outlined in [7], in which both oceanographic, acoustic data and models are merged to minimize an ‘heterogeneous’ cost function. Traditionally, the error of the acoustic prediction is dependent on the water column forecast error and the geometric/geoacoustic parameters accuracy, the latter potentially weak, due to sparsity of bottom data or, for example, to the merely indicative character of the information found on nautical charts or historical databases. It is generally claimed that a decrease in the predicted acoustic signal error is attained only with a decrease in the environmental information error.

Important in acoustic prediction is that the subspace spanned by the acoustic signal is dependent on acoustic modeling constraints. These are essentially threefold: first, computational issues limit the detail of the environmental description; second, the end-user environmental knowledge is often incomplete for the acoustic grid of interest; third, physical inaccuracies may take place due to the numeric approximations applied in solving the acoustic wave equation. From the environmental viewpoint, this implies that, for a given acoustic data set, the simulated acoustic field closest to the acoustic data has to be parameterized by an environment slightly shifted from the real environment, here designated as an ‘equivalent environment’. The structure of the ‘equivalent environment’ can be determined by means of acoustic inversion, which, by definition, finds optimal environmental parametrizations for modeling acoustic fields[8]. Another important issue is that the ocean dynamical model can present biases in its estimates. At this point, if we have at hand sensed ocean data, and watercolumn forecasts, we can envisage three subspaces representing aspects of the same ocean: one for ocean watercolumn/geoacoustic/geometric measures; one for watercolumn forecasts; and one for equivalent environments. The estimation of the future acoustic field can be posed as the estimation of the future equivalent environment. If it is possible to convert quantities from the first two mentioned subspaces into ‘equivalent’ quantities, an optimal estimate of the future acoustic field can be obtained.

This paper presents an acoustic predictor formulated as a Bayesian estimator, which takes into account the environmental model ‘equivalence’ in predicting the acoustic signal, and eventual oceanographic errors/biases. The acoustic signal under prediction is modeled as the realization of a random variable, function of a random environment. The initial information consists of water column measures, oceanographic forecasts, acoustic data and geometric/geoacoustic properties. The posterior PDF of the acoustic signal conditioned on this information is estimated, allowing the direct definition of MMSE, MAP and median estimates, derived from acoustic error cost functions, as implied by the standard Bayesian framework. With realistic acoustic modeling, taking into account that the environmental model will always suffer from slight mismatches in the best case, which requires shifting the true environment for solving the acoustic modeling (forward) problem, the present approach claims that those shifts can be ‘learned’ by solving an inverse problem.

The method is supported by simulations run from measurements and forecasts obtained from the Maritime Rapid Environmental Assessment 2003 (MREA'03) sea trial[9]. Regarding the paper structure, sec. 2 describes the background, sec. 3 presents simulation results, and sec. 4 concludes.

## 2 Bayesian acoustic prediction

Let us consider the problem of predicting the acoustic field  $\mathbf{a}_F(f)$  at an hydrophone array, at frequency  $f$ , and time  $t_F > t_P$ , where  $t_P$  is the present time, associated to an ocean transect as represented in fig. 1. The environment in fig. 1 is a shallow water scenario with characteristics similar to real conditions observed in the MREA'03 sea trial[9], here modeled as a 3 layer-acoustic waveguide. The acoustic observation system is fixed, and composed of an acoustic source and a 6 hydrophone-array.

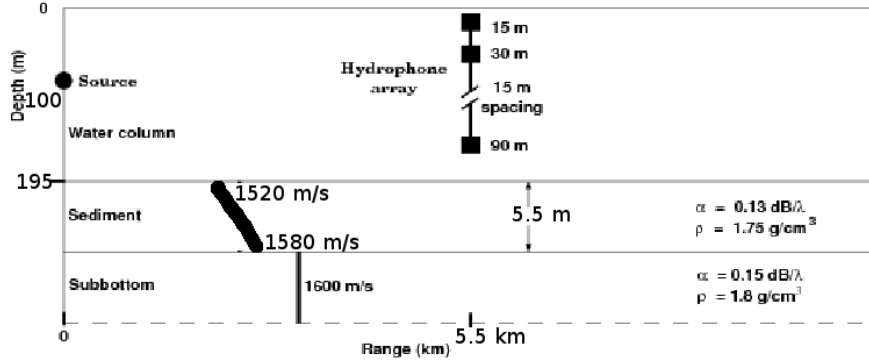


Fig. 1: Acoustic propagation transect used in the simulation.

Figure 2 shows the underlying timeline of the acoustic prediction process, described as follows. At a narrow time window centered on  $t_I$ , an oceanographic model is ini-

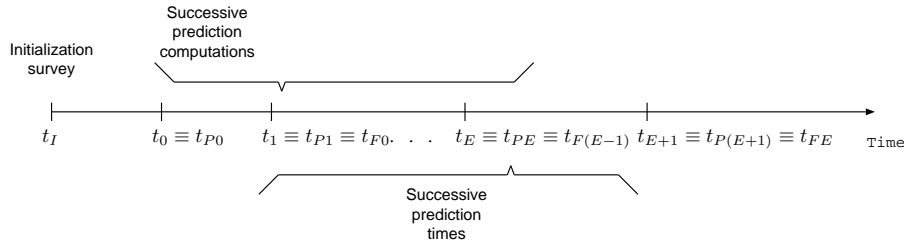


Fig. 2: Acoustic prediction time line. After the initialization of the oceanographic model at  $t_I$ , acoustic and oceanographic samples of the oceanographic area of interest are taken on a regular basis, and the oceanographic model is run for the area, giving forecasts for instants  $t_0, t_1, \dots, t_P$  (present time) and  $t_F$  (future time).

tialized and calibrated for the area of interest with extensive meteo-oceanographic measurements. The model produces forecasts of the water column conditions at times  $t_0, t_1, \dots, t_P, t_F$ . Of interest here are compact representations of these forecasts, namely empirical orthogonal function (EOF) coefficients. To simplify the notation, the forecasts for  $t_0, t_1, \dots, t_P$  are stacked in vector  $\boldsymbol{\omega}$ , and that for  $t_F$  is in vector  $\mathbf{o}_F$ .

Environmental parameter	Notation
Water column SSP 1 <sup>st</sup> EOF coefficient	$m_{w1}$
Water column SSP 2 <sup>nd</sup> EOF coefficient	$m_{w2}$
Water column SSP 3 <sup>rd</sup> EOF coefficient	$m_{w3}$
Sediment compressional speed at water-sediment interface	$m_u$
Sediment compressional speed at sediment-subbottom interface	$m_l$
Sediment thickness	$m_t$
Subbottom compressional speed	$m_p$

Tab. 1: Equivalent environment structure: parameters which vary during acoustic inversion, optimized to model the acoustic data.

At time  $t_0$ , space-time-dense regular oceanographic and acoustic observations start taking place. During a narrow time window centered on each time  $t_k, k = 0, \dots, P$ , the acoustic observation process produces a snapshot  $\mathbf{a}_k(f)$ , where each snapshot contains the complex acoustic signals received on the hydrophones —see fig. 1. The corresponding water column conditions  $\mathbf{w}_k$  are assumed time-invariant during the observation window. The data sets  $\mathbf{a}_k$  and  $\mathbf{w}_k$  are stacked into vectors  $\boldsymbol{\alpha}$  and  $\boldsymbol{\psi}$ , respectively. All the bottom properties are range-independent in the transect and known to the user, forming the vector  $\mathbf{g}$ . Every acoustic data set  $\mathbf{a}_k$  is inverted for the environmental properties, by means of standard acoustic inversion techniques.

In the present work, the acoustic modeling mismatch is created by the EOF representation of the sound speed profiles. The representation is very common in acoustic inversion, to regularize the estimation of sound speed at different depths, and minimize the computation time. The full list of free parameters that describe the environment is shown in tab. 1. They act as degrees of freedom in modeling the acoustic field, and condition the accuracy of the acoustic prediction.

The first step in deriving the estimate  $\hat{\mathbf{a}}_{Fl}(f)$  of the acoustic field is the determination of the posterior PDF of  $\mathbf{a}_{Fl}(f), p(a_{Fl}(f)|\boldsymbol{\omega}, \mathbf{o}_F, \mathbf{g}, \boldsymbol{\alpha})$ , conditioned on all the available data. This PDF can be written as:

$$p(\mathbf{a}_F|\mathbf{c}, \mathbf{g}, \mathbf{o}_F) = \frac{1}{n(\mathbf{c}, \mathbf{g}, \mathbf{o}_F)} \int p(\mathbf{a}_F|\mathbf{m}_F)p(\mathbf{m}_F|\mathbf{c}, \mathbf{g}, \mathbf{o}_F)d\mathbf{m}_F. \quad (1)$$

Notice that the required acoustic field in  $\mathbf{a}_F$  can be generated deterministically with the realization  $\mathbf{m}_F$ , by resorting to the acoustic propagation model at hand, and hence,  $p(\mathbf{a}_F|\mathbf{m}_F) = \delta(\mathbf{a}_F - M(\mathbf{m}_F))$ , where  $\delta$  is the Dirac distribution, and  $M(\cdot)$  represents the environment-to-acoustics transformation carried out by the acoustic propagation model. With the information carried by the posterior PDF of  $\mathbf{a}_F$ , three Bayesian acoustic predictors are then derived[10]:

$$\hat{A}_{MMSE}(l, f) = \int \mathbf{A}_F p(A_F|\mathbf{c}, \mathbf{g}, \boldsymbol{\omega}, \mathbf{o}_F)dA_F; \quad (2)$$

$$\hat{A}_{MAP}(l, f) = \arg \max_{A_F} p(A_F|\mathbf{c}, \mathbf{g}, \boldsymbol{\omega}, \mathbf{o}_F); \quad (3)$$

$$\hat{A}_{MED}(l, f) = \text{median of } p(a_F|\mathbf{c}, \mathbf{g}, \boldsymbol{\omega}, \mathbf{o}_F). \quad (4)$$

True Bayesian estimates of the complex acoustic field should be defined independently for the real and imaginary parts, as pointed out in [10]. Thus, the estimates in (4) are scalar estimates of the field's real or imaginary part, respectively, at each depth-frequency point.

### 3 Simulation

The prediction of the acoustic field  $\mathbf{a}_F(l, f)$  is illustrated in the following, using synthetic noiseless acoustic data generated with collected CTD data and oceanographic forecasts produced for the MREA'03 sea trial[9] by the Navy Coastal Ocean Model[1]. The considered acoustic model was the normal-mode model SNAP[11]. The acoustic system depicted in figure 1 takes observations between Julian day (JD) 151 (June 1<sup>st</sup>) and 175 (June 25<sup>th</sup>) of 2003. The emitted signal is a sum of  $N_{freq} = 10$  equally spaced tones from 540 to 900 Hz. The observations are performed in a regular time grid as shown in figure 2. The aim of the acoustic predictor is to estimate the acoustic field in the hydrophone array —as in figure 1.

At time  $t_{25}$ , the data acquired upto  $t_{25}$  is considered, to predict the acoustic field for all the future time samples. The restriction to the first 3 EOFs in the sound speed profile expansion is the only source of model mismatch. The EOFs were drawn from the CTD SSP data sequentially acquired in a large  $142 \times 87.9$  km area around the Elba Island, in the period May 28<sup>th</sup>–June 25<sup>th</sup>[12]. These 3 EOFs account for 87% of the SSP variance. The oceanographic forecasts were space-time linearly interpolated to the CTD casts, and then, both real and predicted SSPs were linearly interpolated to the regular observation time samples. Figure 3 shows the difference between the projection of the measured and the forecasted profiles onto the first 3 EOFs. In general, the trends

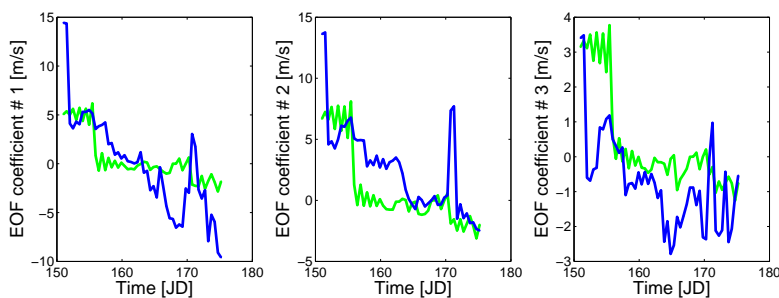


Fig. 3: Difference between the projection onto the first 3 empirical orthogonal functions, of the measured and NCOM predicted sound speed profiles.

of the measured and predicted EOF coefficients coincide. However, the prediction error is highly non-stationary, with average estimation errors of 2.9, 2.4 and 1.3 m/s for the 1<sup>st</sup>, 2<sup>nd</sup> and 3<sup>rd</sup> coefficients, respectively, characterizing the time-averaged bias of the ocean dynamic model. This is not surprising, since NCOM restricts in situ data to remotely sensed sea surface height and temperature, assimilating this data and atmospheric data to a dynamic model, and considering historical relationships between water surface and column properties —being a model suitable for real-time operation.

In the present study, two acoustic predictors are applied. The first is stated as the *standard predictor*. It feeds the acoustic model with the oceanographic forecast of the first 3 EOF coefficients,  $\mathbf{o}_F$ . The second predictor assumes the form of the Bayesian estimators in (4), feeding the model with the ‘equivalent’ environment. The essential difference between the two predictors resides in the statistical assimilation of acoustically inverted data in the estimation process.

The acoustic data was inverted for the parameters in table 1, using the depth-coherent, frequency-incoherent Bartlett processor

$$P(\mathbf{m}_k) = 1 - \sum_{i=1}^{N_{freq}} \tilde{\mathbf{w}}^H(\mathbf{m}_k) \hat{\mathbf{R}}_i \tilde{\mathbf{w}}(\mathbf{m}_k), \quad (5)$$

Equivalent parameter	Search bounds	Resolution
$m_{w1}$	-20, 15	0.097 m/s
$m_{w2}$	-10, 15	0.097 m/s
$m_{w3}$	-8.9, 10	0.097 m/s
$m_u$	1460, 2133	0.37 m/s
$m_l$	1500, 2000	0.37 m/s
$m_t$	1, 8.2	0.061 m
$m_p$	1530, 1800	0.37 m/s

Tab. 2: Characteristics of the search space used in acoustic inversion.

where  $\tilde{\mathbf{w}}$  is an unitary norm acoustic field candidate along the hydrophone array, and  $\hat{\mathbf{R}}_i$  is an estimate of the correlation matrix of  $\mathbf{a}_i$ . During the acoustic inversion, the considered search bounds and resolution for the parameters, are shown in table 2. Both in acoustic inversion and prediction, all the environmental parameters representing geometrical and other geoacoustic properties are fixed to the assumed known values in figure 1.

The statistical processing in the Bayesian estimator is briefly described in the following. As stated by (1), it is required to estimate the future ‘environment’  $\mathbf{m}_F$ , whose information is contained in the posterior PDF  $p(\mathbf{m}_F|\mathbf{c}, \mathbf{g}, \mathbf{o}_F)$ . In the general acoustic prediction problem, each vector  $\mathbf{m}_F$  and  $\mathbf{o}_F$  contains the coefficients of all the EOFs considered relevant for representing the water column variability, which are unconditionally statistically dependent, though uncorrelated. It is expected that the coefficients in  $\mathbf{m}_F$  are also conditionally dependent, with the underlying PDF  $p(\mathbf{m}_F|\mathbf{c}, \mathbf{g}, \mathbf{o}_F)$ . Nevertheless, as a preliminary study, their statistical dependence was neglected here, the same applying to the remaining parameters, allowing the approximation

$$p(\mathbf{m}_F|\mathbf{c}, \mathbf{g}, \mathbf{o}_F) \approx p(m_{w1}|\mathbf{c}, \mathbf{g}, \mathbf{o}_F)p(m_{w2}|\mathbf{c}, \mathbf{g}, \mathbf{o}_F)p(m_{w3}|\mathbf{c}, \mathbf{g}, \mathbf{o}_F)p(m_p|\mathbf{c}, \mathbf{g}, \mathbf{o}_F) \\ \times p(m_u|\mathbf{c}, \mathbf{g}, \mathbf{o}_F)p(m_l|\mathbf{c}, \mathbf{g}, \mathbf{o}_F)p(m_t|\mathbf{c}, \mathbf{g}, \mathbf{o}_F). \quad (6)$$

In estimating the PDF in equation (6), special attention is required for the variables in  $\mathbf{m}_F$ . The primary source of information about this variable is the acoustic inversion process. It is very likely that, in the case in which there is some environmental mismatch, it will be impossible that there exists a vector of equivalent properties that can be used to generate an acoustic field coincident with the measured one. It is expected to exist always some residual ‘acoustic error’, hence rendering impossible the definition of a true equivalent value for  $\mathbf{m}_k$ . Additionally, some environmental properties may not influence the acoustic field observed at particular frequencies (e.g. bottom deep layers properties, at frequencies above 10 kHz). This implies a characterization of the transformation environment-to-acoustics as a many-to-one relation. Also, for computational reasons, the equivalent properties values have to be determined by random search algorithms, which have a probability less than one of finding the environmental values that correspond to the best acoustic fit, for not exploring all the possible environmental combinations, and for working with a discretization that may not consider the best environment in the search space. At last, the acoustic data in real scenarios is noisy, which implies a minimum uncertainty in the estimation process. For these reasons, the environmental outcome from acoustic inversion is described here by only the posterior PDF  $p(\mathbf{m}_p|\mathbf{a}_p)$ . To arrive at the estimate  $\hat{p}(\mathbf{m}_F|\mathbf{c}, \mathbf{g}, \mathbf{o}_F)$  of the PDF in (6), it is necessary to estimate each term on the right-hand of eq. (6). These terms

can be approximated as follows:

$$\begin{aligned}
p(m_{w1}|\mathbf{c}, \mathbf{g}, \mathbf{o}_F) &\approx p(m_{w1}|o_1) \\
p(m_{w2}|\mathbf{c}, \mathbf{g}, \mathbf{o}_F) &\approx p(m_{w2}|o_2) \\
p(m_{w3}|\mathbf{c}, \mathbf{g}, \mathbf{o}_F) &\approx p(m_{w3}|o_3) \\
p(m_p|\mathbf{c}, \mathbf{g}, \mathbf{o}_F) &\approx p(m_p|\mathbf{c}) \\
p(m_u|\mathbf{c}, \mathbf{g}, \mathbf{o}_F) &\approx p(m_u|\mathbf{c}) \\
p(m_i|\mathbf{c}, \mathbf{g}, \mathbf{o}_F) &\approx p(m_i|\mathbf{c}) \\
p(m_t|\mathbf{c}, \mathbf{g}, \mathbf{o}_F) &\approx p(m_t|\mathbf{c})
\end{aligned} \tag{7}$$

The first three densities on the right-hand side of eqs. (7) were approximated as

$$\begin{aligned}
p(m_{w1}|o_1) &\approx p(m_{w1}|\mathbf{a}_p) \\
p(m_{w2}|o_2) &\approx p(m_{w2}|\mathbf{a}_p) \\
p(m_{w3}|o_3) &\approx p(m_{w3}|\mathbf{a}_p)
\end{aligned}$$

For the four last densities in eqs. (7), since the geographical coordinates  $\mathbf{c}$  do not change in time, their estimate, computed at time  $t_P$ , was obtained as a weighted average of previously obtained densities, conditioned on the acoustic data, written for  $m_p$ :

$$p(m_p|c) \approx r \sum_{p=0}^P (1 - P_p(\mathbf{e}_{wP_i})) p_p(m_p|\mathbf{a}_p),$$

where  $P_p(\mathbf{e}_{wP_i})$  and  $p_p(m_p|\mathbf{a}_p)$  are the acoustic cost functions and corresponding posterior densities from acoustic inversion, at time  $t_p$ , and  $r$  is a normalizing term. For the other parameters, the procedure was similar.

The determination of the densities  $p(m_{w_k}|o_1), k = 1, 2, 3$ , was done in two steps: (1) density shape estimation and (2) density mean value estimation. For the shape estimation, the two closest forecasts for the past time are identified, and the corresponding posterior densities from acoustic inversion aligned according to their estimated expected value. Their average defines the shape estimate. For the mean value estimation, an interpolation/extrapolation of the mean values as a function of  $o_k, k = 1, 2$  or  $3$ , was done, for the point  $o_{Fk}, k = 1, 2$  or  $3$ .

Once  $p(\mathbf{m}_F|\mathbf{c}, \mathbf{g}, \mathbf{o}_F)$  is estimated, the acoustic signal corresponding to each outcome of  $\mathbf{m}_F$  is computed by forward modeling. Afterwards, this ensemble of acoustic signals is binned, and each bin weighted according to  $p(\mathbf{m}_F|\mathbf{c}, \mathbf{g}, \mathbf{o}_F)$ , to produce an histogram which is the estimate of  $p(A_F|\mathbf{c}, \mathbf{g}, \boldsymbol{\omega}, \mathbf{o}_F)$ . At the end, the predicted acoustic field emerges as a trivial application of (4) to the obtained  $p(A_F|\mathbf{c}, \mathbf{g}, \boldsymbol{\omega}, \mathbf{o}_F)$ .

### 3.1 Results

This section presents the results of acoustic prediction obtained with the Bayesian and the standard acoustic predictors. It starts by illustrating the steps of the Bayesian predictor. In the first step, acoustic inversion, the obtained results, using the acoustic inversion software SAGA[13], are shown in fig. 4. As we can see, the equivalent environment  $\mathbf{m}_p$  differs from the true one,  $\boldsymbol{\theta}$ . An environmental error measure  $\epsilon$  was defined, in order to characterize the impact of the environmental mismatch in the determination of the equivalent environment, as follows:

$$\epsilon = \text{acos}(\boldsymbol{\theta}^T \mathbf{m}_p),$$

and is plotted in fig. 5. From this figure, we can infer that: 1) low acoustic misfits are in general associated to low environmental misfits. This happens when the environmental

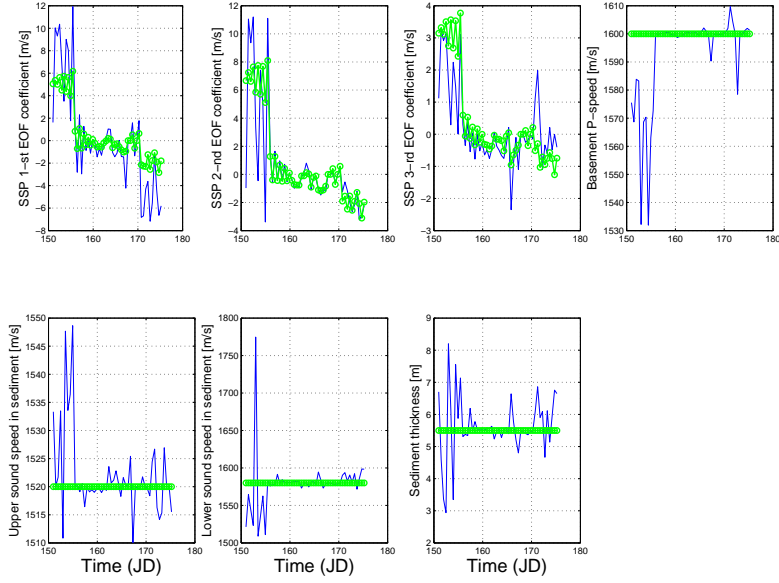


Fig. 4: Acoustic inversion results for the seven parameters in tab. 1: true (green) and estimated (blue) environmental parameters.

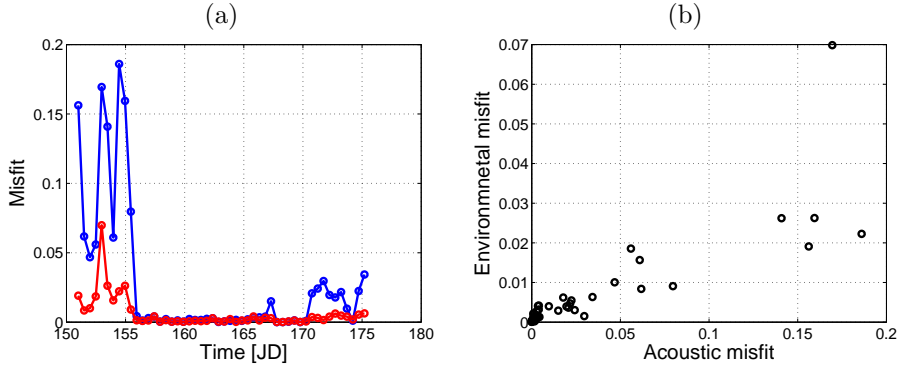


Fig. 5: Environmental (red) and acoustic (blue) misfits, at each inversion step (a) and acoustic vs. environmental misfit (b).

mismatch present in the inversion process is low, and is an indicator of the unicity of the acoustic field with respect to the environmental properties associated to the measured field. 2) The exceptions to the trend, like the one verified for the points 0.06 and 0.08 for the acoustic misfit, and 0.02 and 0.01 for the environmental misfit, indicate that the relation between the misfits is not a direct relation, which is also a consequence of the non-direct relation between environmental properties and acoustic field properties.

The second step in the acoustic prediction method, the estimation of the densities in eq. (7), is illustrated by the results shown in figs. 6, 7 and 8. Finally, and taking into account eq. (6), for the third step, the acoustic field is computed for each non-zero of a thresholded version of  $\hat{p}(\mathbf{m}_F|\mathbf{c}, \mathbf{g}, \mathbf{o}_F)$ , binned in a histogram, and each bin weighted according to the corresponding environmental value in  $\hat{p}(\mathbf{m}_F|\mathbf{c}, \mathbf{g}, \mathbf{o}_F)$ . This procedure was done for the real and imaginary parts, individually, of the field at each



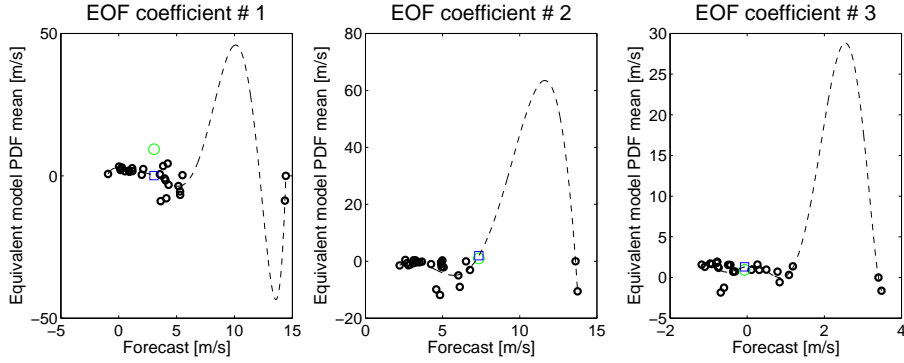


Fig. 6: Future environmental posterior densities mean estimates, for the EOF coefficients: true (square) and estimated (blue circle) means, by a 7<sup>th</sup>-order polynomial fit. The fit considered the oceanographic forecast EOF coefficients as abscissae (black circles).

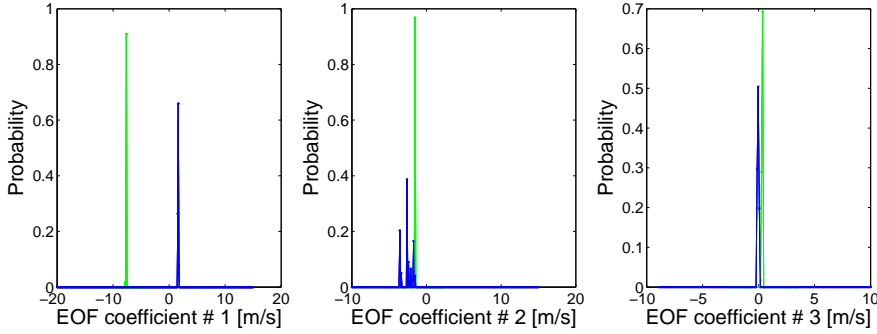


Fig. 7: Future environmental posterior densities estimates, for the EOF coefficients: true (green) and estimated PDFs, with the shape estimated as an average shape of neighbor (associated to the 2 oceanographic forecasts closest to the oceanographic forecast for  $t_F$ ) densities, and the means taken as the estimates shown on fig. 6.

hydrophone depth and frequency. In fig. 9, we can see the acoustic estimates obtained by the Bayesian procedure, along with the true values and the estimates obtained by the standard approach. The average error of the standard and Bayesian approaches are  $4.6e-4$  and  $3.9e-4$  (median-estimate), respectively, for the real part, and  $4.3e-4$  and  $3.1e-4$  (MAP-estimate), respectively, for the imaginary part.

The estimates errors for the standard and Bayesian approaches, corresponding to the fields predicted for Julian time  $\geq 164$  are plotted in fig. 10. As we can see in the figure, the present Bayesian method is a fair alternative to the standard approach, with a comparable estimation error. In the presented results, the scenario is in fact highly favorable to the standard approach, in that all the environmental parameters apart from the water column coincide in the generation of the acoustic signals, and in the forecast of the acoustic field.

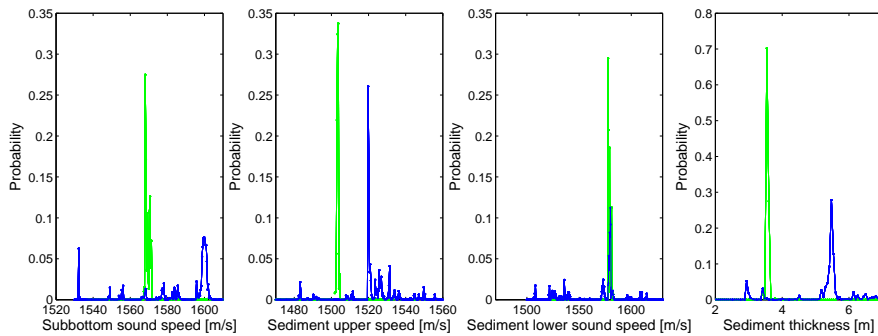


Fig. 8: Future environmental posterior densities estimates for bottom parameters: true (green) and estimated PDFs, with the shape estimated as a weighted average of all the past posterior densities from acoustic inversion.

## 4 Conclusions

A Bayesian approach for the prediction of the acoustic field has been presented, in which the acoustic model is calibrated with acoustic observations at past and present time. This calibration, necessary to compensate for modeling mismatches, was used to compensate for the modeling error of the water column sound speed, which uses only 3 empirical orthogonal functions in its representation. In the scenario supporting the numerical results, an ocean transect with a fixed acoustic system, the acoustic inversion results show that the environmental model, outcome from acoustic inversion, is fairly variable, even for the bottom parameters, which are constant in time. The acoustic inversion step allows to track this variability, and use it in the prediction of the future acoustic fields. The results are still comparable to the ones obtained by using a standard predictor, in which the acoustic forecast is the output of an acoustic propagation model parameterized by a water column forecast and the remaining parameters coincident with the ones used to generate the synthetic acoustic ‘data’. In this point, we can envisage an extreme sensitivity of the standard approach to the environmental knowledge respecting non-water column properties, by comparison to the present approach, which estimates the relevant unknown properties, and will be studied in the future.

## Acknowledgements

This work was partially supported by the project WEAM (PTDC/ENR/70452/2006), the scholarship SFRH/BD/9032/2002, from FCT, Portugal, and the EU OAEx Marie Curie FP7 230855 Program. Thanks are due to all the people involved in the MREA’03 Sea Trial, with Dr. Emanuel Coelho as scientist in charge.

## References

- [1] P.J. Martin. Description of the Navy Coastal Ocean Model version 1.0. report NRL/FR/7322-00-9962, Naval Research Laboratory, 2000.
- [2] F.B. Jensen, W.A. Kuperman, M.B. Porter, and H. Schmidt. *Computational Ocean Acoustics*. American Institute of Physics, 1993.
- [3] A.R. Robinson and the LOOPS Group. Realtime forecasting of the multidisciplinary coastal ocean with the Littoral Ocean Observing and Predicting System

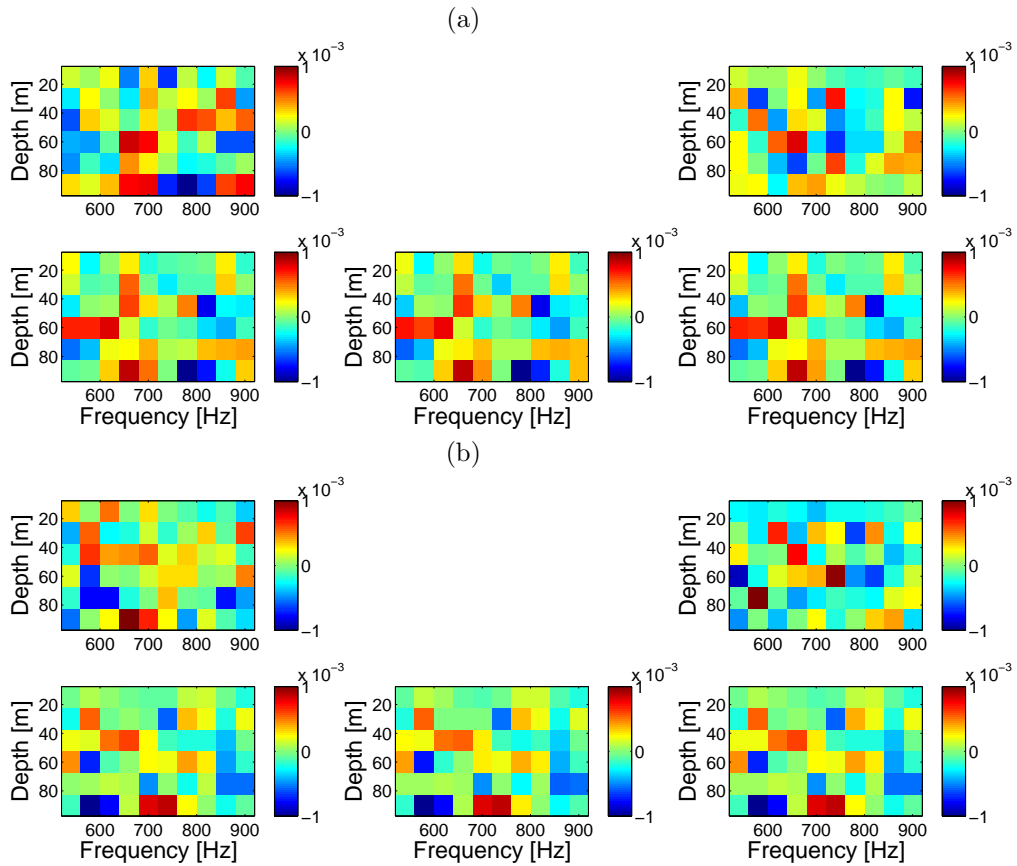


Fig. 9: Real (a) and imaginary (b) parts of the predicted acoustic pressure at the hydrophone depths and frequencies used in the acoustic inversion. The true acoustic pressure is in the top left figures in (a) and (b), the estimate by the standard approach, in the top right figures in (a) and (b), and the one by the present Bayesian approach, in the bottom figures in (a) and (b), for MAP, MMSE and MED estimates, from left to right, respectively.

(LOOPS). In *preprint volume of the Third Conference on Coastal Atmospheric and Oceanic Prediction and Processes, 3–5 November 1999, New Orleans, LA*. American Meteorological Society, Boston, MA, 1999.

- [4] A.R. Robinson. *Forecasting and Simulating Coastal Ocean Processes and Variabilities with the Harvard Ocean Prediction System*, pages 77–100. AGU Coastal and Estuarine Studies Series. American Geophysical Union, 1999.
- [5] A.R. Robinson and P.F.J. Lermusiaux. Prediction systems with data assimilation for coupled ocean science and ocean acoustics. In *Sixth International Conference on Theoretical and Computational Acoustics (ICTCA)*, pages 325–342, Honolulu, HI, 11 August, 2003.
- [6] P.F.J. Lermusiaux, C.-S. Chiu, G.G. Gawarkiewicz, P. Abbot, A.R. Robinson, R.N. Miller, P.J. Haley, W.G. Leslie, S.J. Majumdar, A. Pang, and F. Lekien. Quantifying uncertainties in ocean predictions. *Oceanography, Special issue on*

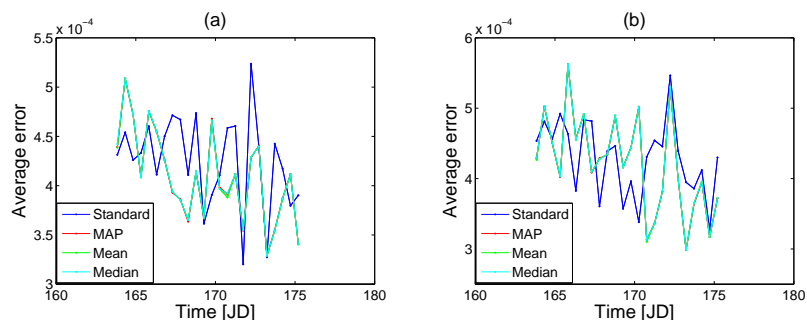


Fig. 10: Acoustic field estimate error at times  $\geq$  Julian day 164, obtained by the standard and Bayesian approaches: real (a) and imaginary (b) parts of the acoustic pressure.

“*Advances in Computational Oceanography*”, T. Paluszkiwicz and S. Harper, Eds., 19(1):92–105, 2006.

- [7] P.F.J. Lermusiaux. Uncertainty estimation and prediction for interdisciplinary ocean dynamics. *J. Computational Physics, Special issue on “Uncertainty Quantification”*, J. Glimm and G. Karniadakis, Eds., 2006.
- [8] Y.H. Goh, P. Gerstoft, and W.S. Hodgkiss. Statistical estimation of transmission loss from geoacoustic inversion using a towed array. *J. Acoust. Soc. America*, 122:2571–2579, 2007.
- [9] S.M. Jesus, C. Soares, and A.J. Silva. Acoustic Oceanographic Buoy testing during the Maritime Rapid Environmental Assessment 2003 sea trial. Report 04/03, SiPLAB, University of Algarve, Faro, 2003.
- [10] Steven M. Kay. *Fundamentals of statistical signal processing: estimation theory*. Prentice-Hall, Inc., Upper Saddle River, NJ, USA, 1993.
- [11] F.B. Jensen and M.C. Ferla. Snap: The saclantcen normal-mode acoustic propagation model. Technical Report SM-121, SACLANT Undersea Research Centre, La Spezia, Italy, 1979.
- [12] N. Martins, C. Soares, and S. Jesus. Environmental and acoustic assessment: The aob concept. *Journal of Marine Systems*, 69:114–125, 2008.
- [13] Peter Gerstoft. Saga user manual 5.4., 2007.